Available online at www.sciencedirect.com
ScienceDirect
Journal of Sound and Vibration 299 (2007) 559–574
JOURNAL OF SOUND AND VIBRATION
www.elsevier.com/locate/jsvi

A coherent model for predicting noise reduction in long enclosures with impedance discontinuities

P.M. Lam[a], K.M. Li[b,*]

[a]Department of Mechanical Engineering, The Hong Kong Polytechnic University, Hung Hom, Hong Kong
[b]Ray W. Herrick Laboratories, School of Mechanical Engineering, Purdue University, West Lafayette, IN 47907-2031, USA

Received 3 October 2005; received in revised form 23 May 2006; accepted 23 June 2006
Available online 9 October 2006

Abstract

A theoretical model has been developed for the prediction of sound propagation in a rectangular long enclosure with impedance discontinuities. Based on the image-source method, the boundaries are assumed to be geometrically reflective. An infinite number of image sources are generated by multiple reflections. The sound pressure of each image is obtained by an approximate analytical solution, known as the Weyl-van der Pol formula. The total sound field is then calculated by summation of the contribution from all images. The phase information of each image and the phase change upon reflection are included in the model. A single change of impedance in a two-dimensional duct is focused on as the fundamental problem of the current study. The diffraction effect at the impedance discontinuity is proved to be insignificant, and it is ignored in the formulation. On the assumption that the diffraction effect is not important, the investigation is moved on to a rectangular long enclosure. Measurements are conducted in two model tunnels to validate the proposed prediction model. The predictions are found to give good approximations of the experimental results. The theoretical model serves as the first attempt to optimize the position and pattern of sound absorption materials in a long enclosure, such as an underground railway station or a building corridor, for the reduction of noise and improvement of sound quality.

1. Introduction

Much attention in recent research has been devoted to the sound propagation in long enclosures with homogeneous surfaces. The acoustical properties of the four boundaries remain the same along the length of the enclosure. A common practice for noise abatement in a long enclosure is to line the boundary surfaces with sound absorption materials. However, it will not be economical, nor can it achieve maximum efficiency, if the sound absorption materials are installed along the entire length of the enclosure. It is necessary to optimize the pattern, the amount, and the location of the absorption materials. For example, patches of absorption material can be placed on the ceiling at certain intervals. A theoretical model can assist the design of such an arrangement of absorption materials.

*Corresponding author. Tel.: +1 765 494 1099; fax: +1 765 494 0787.
E-mail address: mmkmli@purdue.edu (K.M. Li).

0022-460X/$ - see front matter © 2006 Elsevier Ltd. All rights reserved.
doi:10.1016/j.jsv.2006.06.071

Computation of the sound field in a room with mixed-impedance surfaces can be traced back to the classic theory. The Sabine absorption coefficient [1] was an area-weighted value of the surfaces in a room. It was frequently used to calculate the reverberation time with the assumption of a diffuse sound field. Kang [2] presented a radiosity model for the prediction of sound field and acoustic indices in a long enclosure. It was an energy approach, and the phase information of all reflected waves was ignored in the calculation.

The attenuation of noise by duct silencers is a similar problem to that of the propagation of sound in a tunnel or corridor. Although the dimension and boundary conditions are different, some of the theoretical principles for ducts are also useful for long spaces. The mode-matching technique was adopted by Mechel [3] and Somraz et al. [4] to account for diffraction at the duct silencer's terminations. Astley and Eversman presented a finite-element formulation [5] and the weighted residual method [6] for finite-length silencers with mean gas flow. These prediction schemes required considerable computational effort, and it was difficult to track the modes in the first method.

Tester [7] compared ray theory and modal predictions of the sound field from a line source in a two-dimensional duct with zero flow and locally reacting walls. He concluded that the ray models were "surprisingly" accurate. The advantages of ray models were their simplicity and versatility. Cummings [8] developed a hybrid mode/ray model for a two-dimensional duct with a length of soft walls and rigid inlet and outlet sections. Cummings suggested that the diffraction effect was not important when the frequency was sufficiently high. The formulation did not account for the diffraction at the inlet and outlet sections of the silencer. An alternative approach was adopted by other researchers, who investigated the absorption effect of periodic absorptive strips [9–13]. Both scattering and absorption effects were expressed by a single absorption coefficient when strips of absorbent material were arranged periodically on a surface.

In our earlier study [14], a coherent model based on the image-source method was validated for predicting the sound field in long enclosures with homogeneous impedance surfaces. The same approach will be used in the present study. Further, a-empirical model by De Jong et al. [15] is incorporated into the coherent model to account for the diffraction at the impedance discontinuity. The numerical model will be applied to a two-dimensional duct first. The diffraction effect due to the impedance discontinuity will be critically examined to determine its importance as compared with the direct and reflected sound fields in long enclosures. Next, the coherent model will be extended to a long rectangular duct. Experimental validations of the coherent model for the propagation of sound in a rectangular duct will also be presented. Finally, the coherent model will be used to conduct a numerical study for assessing the effectiveness of the noise reduction by varying the pattern, the amount, and the location of the absorption materials installed at the walls of a tunnel.

2. Theory

2.1. Single impedance discontinuity in two parallel horizontal planes

The formulation for the prediction of outdoor sound propagation over an impedance discontinuity proposed by De Jong et al. [15] is incorporated into the coherent model to evaluate the sound field in a two-dimensional duct. The geometry of the enclosure is shown in Fig. 1. There is an impedance change from Z_{G1} to Z_{G2} at $y = y_D$ on the lower horizontal surface. This means the region $y < y_D$ on the lower plane has a specific normalized impedance of Z_{G1}, and that of the region $y > y_D$ is Z_{G2}. The remaining boundary surfaces have arbitrary impedance. The source S_0 is placed at $(0, 0, z_S)$, and the receiver R at (x_R, y_R, z_R), where $y_R > y_D$.

In the image-source method, the boundaries of an enclosure are assumed to be removed, leaving an infinite number of images behind. Fig. 1 shows the image sources formed by multiple reflections from two parallel planes. The coordinates of the image sources are $(0, 0, z_n)$, where $n = -\infty \cdots \infty$. The images are conveniently grouped into matching pairs. A typical pair of images is shown in Fig. 2. It contains two image sources: S_j and S_{-j-1}, where $j = 0, 1, \ldots, \infty$. The contribution of sound pressure of each pair of images is composed of three parts, represented by waves traveling through different paths: the direct path (r_1), the reflected path (r_2), and the diffracted path (r_3). The lengths of the paths are determined by simple geometrical considerations. The diffracted path is determined by establishing the shortest distance traveled from the image source S_j to the edge of the impedance step, and then to the receiver. The point at which it hits the impedance step is called the diffraction point D_j. The reflection point M_j is the point at which the image S_j is reflected from the ground

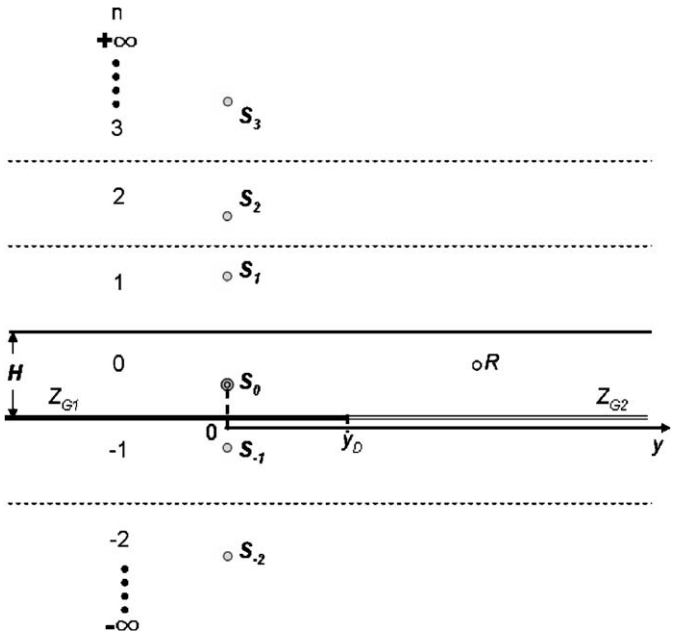

Fig. 1. Formation of images in two parallel horizontal planes.

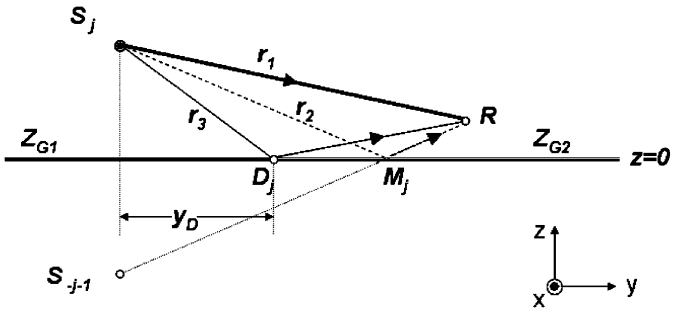

Fig. 2. Schematic diagram of an image pair.

surface. The sound field contributed by the pair of image sources can be written as

$$P_D(j) = P_j + P_{-j-1} + P_{\text{diff}}, \tag{1}$$

where P_j and P_{-j-1} are the respective sound fields due to the pair of image sources and P_{diff} is the contribution due to the diffraction of sound at the edge of the impedance.

The sound field of an image source S_n is given by

$$P_n = Q_n \frac{e^{ikd_n}}{4\pi d_n} \quad \text{for } n = -\infty \cdots \infty, \tag{2}$$

where k ($\equiv\omega/c$) is the wave number, ω is the angular frequency, c is the speed of sound in air, d_n is the distance of the image source n from the receiver, and Q_n is the combined complex wave reflection coefficient associated with the image source n. The computation of Q_n is dependent on the number of times n that a particular ray reflects from the different impedance surfaces. The details for computing Q_n can be found in Ref. [14]. By setting $n = j$ and $n = -j-1$, respectively, in Eq. (2), the values of P_j and P_{-j-1} can be calculated directly.

The determination of the diffraction term P_{diff} is straightforward and details are given in Ref. [15]. In fact, the diffraction term has proved to be a less important component in long enclosures, so that its omission does

not lead to a significant error in calculating the total sound field. More details to justify the exclusion of the diffraction will be given in the next section.

2.2. The diffraction term in long enclosures

The diffraction of sound at an impedance discontinuity in outdoor sound propagation has been studied widely, see for example Ref. [16]. It was found that the diffraction effect was pronounced at near-grazing incidence if there was only a single boundary surface with an impedance discontinuity. In the presence of another boundary surface parallel to the first one, Cummings [8] suggested that the diffraction effect was not important when the frequency was sufficiently high. Cummings used this assumption to develop a hybrid mode/ray model for calculating the attenuation of sound in a duct silencer. Ignoring the diffraction effect in the present ray model, Eq. (1) can be reduced to

$$P_D(j) = P_j + P_{-j-1}. \tag{3}$$

To confirm the validity of this assumption, we compared the predicted sound fields with and without the diffraction term in a prior numerical study [17]. The geometry is the same as the one shown in Fig. 1. The distance between the two horizontal planes is 4 m. The upper horizontal plane and the region $y < y_D$ of the ground are perfectly hard, i.e., $Z_{G1} = 1$. The remaining area of the ground ($y > y_D$) has an impedance of Z_{G2}. It is assumed from the definition of the diffraction coefficients that the amount of change of impedance and the ratio of the area in the two regions are the major factors determining their contribution to the prediction results. Therefore, different values of effective resistivity are used in the one-parameter model [18] to simulate the normalized impedance Z_{G2}. The proportion of the ground with impedance Z_{G1} and Z_{G2} is also varied in the analysis.

The source and the receiver, which are separated by a horizontal distance of 50 m, are placed equidistant from the lower and upper horizontal planes (i.e., 2 m from the surfaces). Comparisons are made on the prediction of excess attenuation (EA) to investigate the diffraction effect. The EA is defined as the ratio of the total sound field to the direct field. The predictions are made with Eqs. (1) and (3) accordingly.

First we compare the EA when the diffraction effect is included and excluded correspondingly. The impedance Z_{G2} is calculated with an effective flow resistivity of 100, 500, and 1000 kPa s m^{-2} in the one-parameter model. Generally speaking, a lower value of flow resistivity represents a more absorptive surface. The impedance of the ground changes at $y = 35$ m. The overall differences for the three cases are 0.12, 0.01, and 0.02 dB, respectively. Next, the percentage of the harder ground is varied. The impedance change occurs at $y = 10$, 20 and 40 m, respectively. The numerical results represent three different ratios of hard/soft ground surfaces, but the effective flow resistivity remains unchanged at 100 kPa s m^{-2}. The overall differences for the three cases are 0.12, 0.17, and 0.22 dB, respectively.

Thus it is reasonable to assume that the diffraction terms do not have a notable influence on the computation of the total sound field in a two-dimensional duct. The diffraction effect is expected to be small and submerged by multiple reflections in a long enclosure. Although the diffraction effect is more pronounced in near-grazing propagation over ground, it is less important in an enclosed space where the sound field is dominated by the direct and multiple reflected waves. As a result, Eq. (3) will be used in subsequent calculations in preference over Eq. (1) because of the apparent reduction in computational time for calculating the total sound field.

As a further validation of the simplified model, predictions are compared with those computed by an integral model. The integral model is based on the Thomasson integral method [19] subsequently modified by Ramussen [20]. In fact, Stinson and Daigle [21] used this integral approach to investigate the propagation of surface waves over a ground with an impedance discontinuity. In a recent study, Li and Wong [22] demonstrated that the integral method was effectively an approximate boundary element formulation. In Ref. [23], Chan extended the integral model that allowed the computation of a sound field in a two-dimensional duct. We use his numerical results to compare with those obtained by the coherent model. In the following numerical comparisons, the two-dimensional duct is modeled by two horizontal planes which are separated by a perpendicular distance of 2 m. The source and receiver are placed at heights of 1 and 0.5 m above the bottom plane respectively and separated by a horizontal distance of 2 m. In the first set of simulations, the

two-dimensional duct has impedance boundaries at the first meter, and hard boundaries at the next meter. In the second set of calculations, the relative positions of the impedance/hard boundaries are reversed, i.e., the two-dimensional duct has hard boundaries at the first 1 m, and impedance boundaries at the next. The impedance of the surface is characterized by Attenborough's two-parameter model [24]. In all numerical simulations, the parametric values of 120 kPa s m^{-2} and 100 m^{-1} are used respectively for the effective flow resistivity and the effective rate of change of porosity with depth.

Fig. 3 shows a comparison of the predicted EA, which is defined as the ratio of the total sound field, P_T, to the direct field, P_0:

$$\mathrm{EA} = 20\ \log(P_T/P_0). \tag{4}$$

The prediction with the modified integral formulation is displayed in Figs. 3(a) and (b) (Figs. 4c,d and 5c,d in Ref. [23]), and that with the proposed coherent model is shown in Figs. 3(c) and (d), respectively. It is worth noting that the diffraction effects have been included in the integral formulation but they are ignored in the coherent model. The results calculated with these two models agree with each other reasonably well. Neglecting the diffraction terms in the coherent model, we simplify the procedures for computing the sound fields considerably. However, the essential phase information has been retained that leads to accurate predictions of sound field in a long enclosure of a two-dimensional duct.

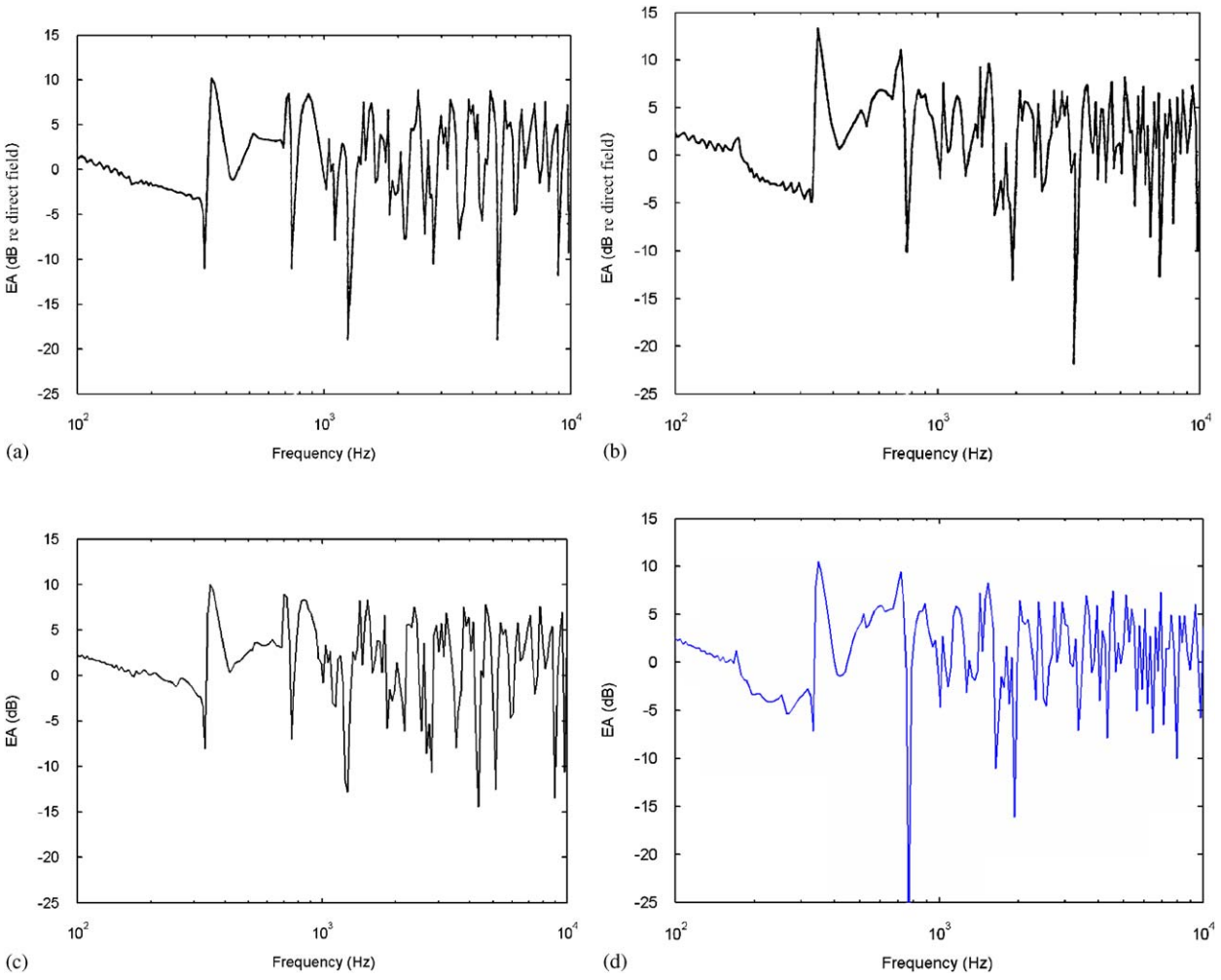

Fig. 3. Plots of excess attenuation for: (a,b) prediction from Chan's model; (c,d) prediction from the coherent model.

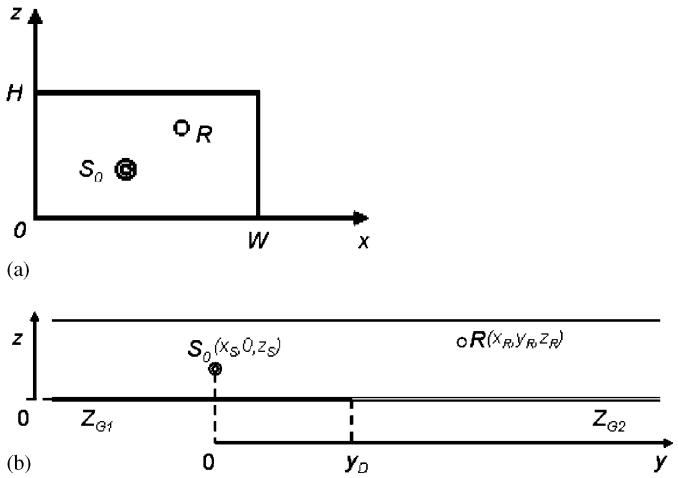

Fig. 4. Schematic diagrams for a long enclosure with single impedance discontinuity: (a) cross-sectional view and (b) side view.

2.3. Single impedance discontinuity in a long enclosure

Next, the coherent model will be extended to the case of a long enclosure with a rectangular cross-section. The contribution of diffraction to the total sound field in a two-dimensional duct is shown to be less important in the previous section. Hence, it is reasonable to assume that the diffraction effect will be even more insignificant with the introduction of two vertical homogeneous boundaries. In other words, diffraction is ignored in the computation for the sound fields in the three-dimensional case. The geometry of the long enclosure is shown in Fig. 4. Essentially, the region $y<y_D$ on the lower plane has an acoustic impedance of Z_{G1}, and that of the region $y>y_D$ is Z_{G2}. The source S_0 is placed at $(x_S, 0, z_S)$, and the receiver R at (x_R, y_R, z_R) where $y>y_D$.

As mentioned before, the walls of an enclosure are assumed to be removed in the image-source method, leaving an infinite number of images behind. The total sound field can be obtained by the summation of the contribution from all image sources as follows:

$$P_{\text{total}} = \frac{1}{4\pi}\sum_{m=0}^{\infty} Q_m \frac{e^{ikd_m}}{d_m}, \tag{5}$$

where k ($\equiv\omega/c$) is the wave number, ω is the angular frequency, c is the speed of sound in air, d_m is the distance of the image source m from the receiver, and Q_m is the combined complex wave reflection coefficient associated with the image source m. The value of Q_m is dependent on the number of times m reflects from the different impedance surfaces. The computation of Q_m is given in Ref. [14] and thus will not be repeated here. Nevertheless, one of the major tasks is to find out the number of times an image hits the boundaries with different absorption coefficients. We remark that the incoherent model (see, for example, Ref. [24]) may also be used straightforwardly since the diffraction term has been excluded in the computation of the total sound fields.

The impulse response of sound pressure can be computed by taking the inverse Fourier transform of the frequency response. The decay curve is then generated by a reverse-time integration of the squared impulse response. The reverberation time is determined from the decay curve. The numerical predictions of noise reduction and early decay time (EDT) from both the coherent and incoherent models are compared with measurements in the following sections.

3. Experimental validations

Indoor and field measurements were conducted to validate the proposed coherent model. Two sets of experimental data were collected in two model tunnels. Details of the experimental arrangements are given below.

3.1. Small-scale model tunnel in an anechoic chamber

A hard plywood model tunnel with open ends was set up in an anechoic chamber. It was 4.8 m long and had a rectangular cross-sectional area of $0.8 \times 1.2\,m^2$. The plywood was carefully varnished to prevent any leakage of sound, such that the boundaries of the model tunnel were assumed to be perfectly hard surfaces. A Tannoy driver fitted with a tube of length 1 m was used as a point source generating white noise. The receiver used in the measurement was a Brüel & Kjær type 4942 pre-polarized diffuse field 1/2 in condenser microphone. It was fitted with a Brüel & Kjær type 2671 Deltatron pre-amplifier. A PC-based maximum length sequence system analyzer [25] was used both as the signal generator for the source and as the analyzer for subsequent data processing.

The entire lower horizontal plane was covered initially with a 3-cm thick layer of fiberglass. The sound pressure levels (SPLs) at different positions of the source and receiver were measured. Afterwards, only part of the surface was covered with fiberglass, so that $y_D = 1.8$ m. The SPLs at the same positions were measured again. The relative SPL is defined as the SPL when the plane is entirely covered with fiberglass, with reference to the SPL when only part of the surface is covered with fiberglass. The configuration of the model tunnel is shown in Fig. 4, in which the impedance of the fiberglass is represented by Z_{G2}.

To characterize the acoustic impedance of the fiberglass used in the experiments, prior measurements were conducted in the anechoic chamber, where the same sheet of fiberglass was laid on a flat ground. By measuring the EA of the sound propagation over the flat surface of the fiberglass, its acoustic impedance could be determined. It was found that the Delaney and Bazley model with a hard-back layer [26] was sufficient to give a reasonable representation of the acoustic impedance of the 3-cm fiberglass laid on a rigid ground. The best-fit parametric value for the effective flow resistivity is $40\,kPa\,s\,m^{-2}$. Fig. 5(a) displays a typical predicted spectrum of the EA compared with the measured results. It shows that the use of the Delaney and Bazley model with a hard-back layer leads to good prediction of the measured EA. Although other more sophisticated theory may give a better approximation of the impedance of fiberglass, the Delaney and Bazley model is employed since it can be incorporated into the coherent model directly, reducing the amount and complexity of controlling parameters. On the other hand, the absorption coefficient of the fiberglass used in

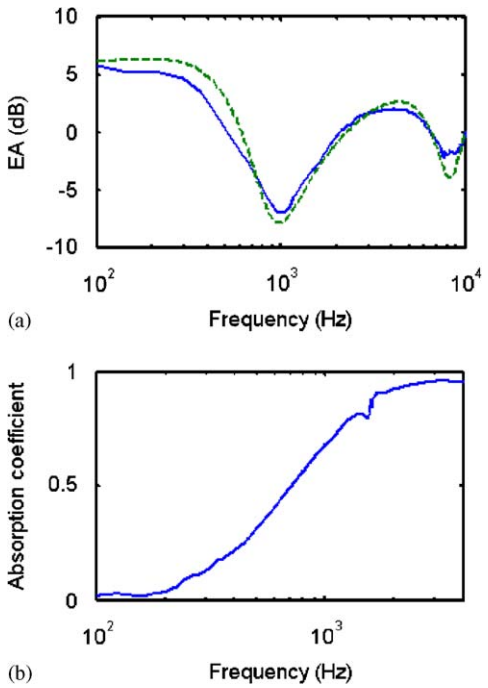

Fig. 5. Characterization of impedance of fiberglass—excess attenuation against frequency. (a) Measurement (—); prediction (----) and (b) plot of absorption coefficient against frequency.

the incoherent model was measured with a standard impedance tube. The results at different frequencies are shown in Fig. 5(b). It is noted that this set of absorption coefficients can also be used in the radiosity model, since the phase information is again ignored. The relationship between the incoherent model and the radiosity model is available in Ref. [2].

In the model tunnel, the source and receiver were set at 0.13 and 0.67 m above ground, respectively. Fig. 6 shows the relative SPL related to different 1/3-octave bands when the source and receiver were separated by 2, 2.5, 3, and 3.5 m, respectively. The source was placed 0.2 m from one of the vertical walls, and the receiver was placed equidistant to both walls. Predictions from the coherent model were compared with those from the incoherent model, and with the measurements. It is found that the coherent model can give a reasonably accurate prediction of the measurements but the incoherent model can only give an average level of the sound fields. There is a 'dip' at 630 Hz in Fig. 6(b), and one at 800 Hz in Fig. 6(d). The coherent model can predict the positions of the dips accurately but the incoherent model is unable to predict these dips. In these sets of measurements, the average error of the coherent model is 1.19 dB, and that of the incoherent model is 3.17 dB. Generally speaking, the coherent model usually gives a more accurate prediction of the sound fields than the incoherent model. These results are not shown here for conciseness.

Fig. 7 shows the measured and predicted EDT spectra at two other source–receiver locations. Fluctuations of EDT are observed due to the interference effect. For example, in Fig. 7(b), the model can predict the down slope between 250 and 500 Hz, followed by a peak at 630 Hz. The average error of the coherent model is 0.1 s. On the other hand, the incoherent prediction is simply a straight line. Interference effects cannot be approximated by the incoherent model.

Some discrepancies between the measurements and predictions according to the coherent model are found in Figs. 6 and 7. One major factor was due to the insufficient length of the small-scale tunnel in the anechoic chamber. The edges of both ends of the model tunnel caused diffraction and scattering effects on the sound field. Experimental results obtained at other source–receiver combinations are similar to those shown in Figs. 6 and 7. It is also worth noting from the measurements and predictions that when the entire plane is

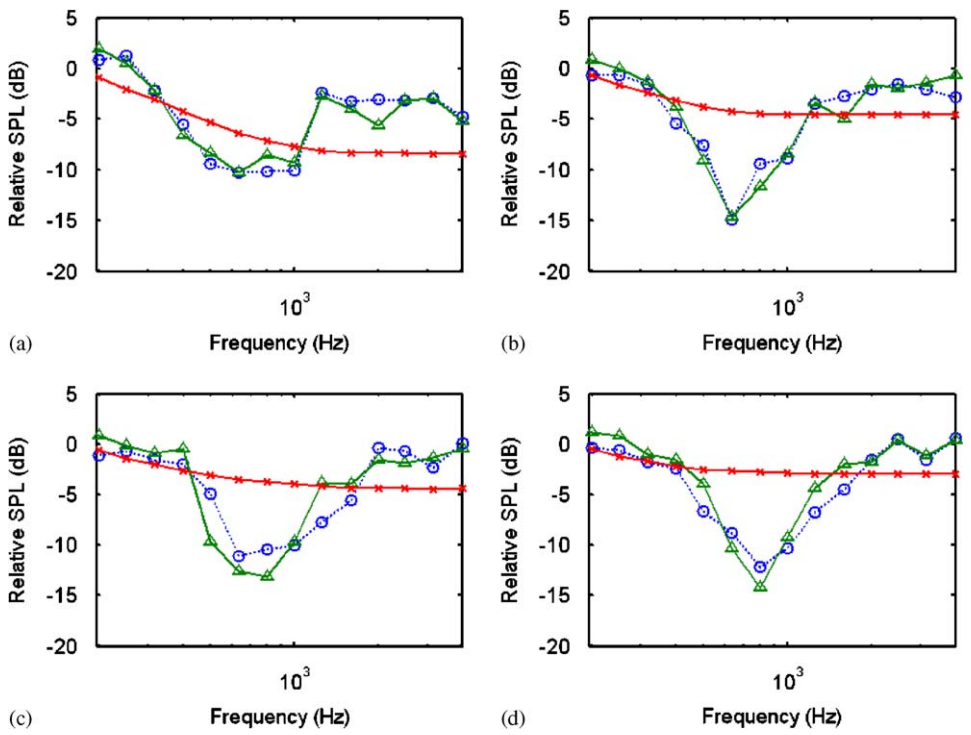

Fig. 6. Comparison of measured and predicted relative SPL in model corridor in anechoic chamber. Source height = 0.13 m, receiver height = 0.67 m, impedance discontinuity at 1.8 m. Measurement: circles; coherent prediction: triangles; incoherent prediction: crosses. Source–receiver distance: (a) 2 m; (b) 2.5 m; (c) 3 m; (d) 3.5 m.

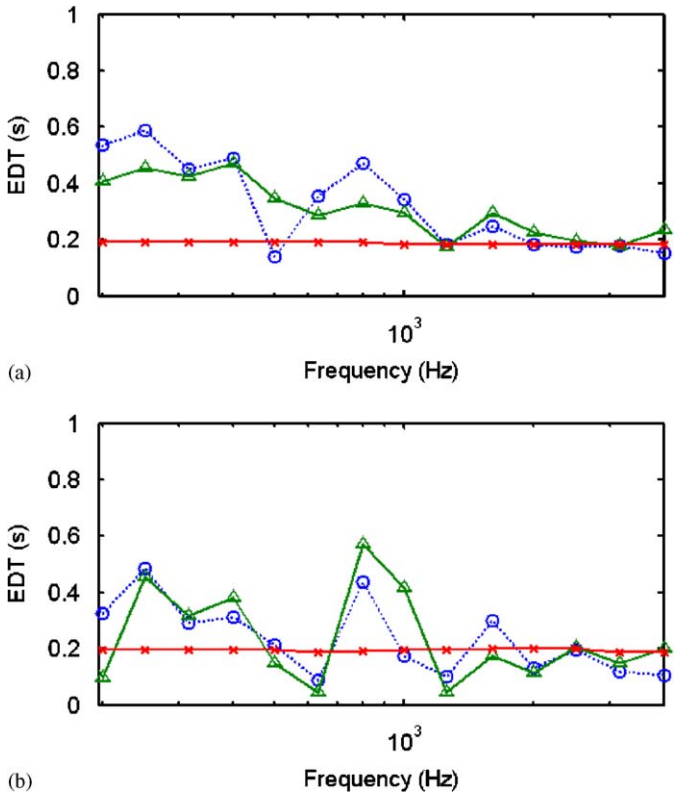

Fig. 7. Measured and predicted EDT spectra in model corridor in anechoic chamber. Change of impedance at $y = 1.8$ m. Measurement: circles; coherent prediction: triangles; incoherent prediction: crosses. (a) Source at (0.2, 0, 0.13), receiver at (0.2, 2, 0.67); (b) source at (0.2, 0, 0.13), receiver at (0.4, 2.5, 0.67).

covered with fiberglass, an extra noise reduction up to 10 dB can be achieved at a particular frequency range. The idea of noise reduction by strategic positioning of sound absorption materials in tunnels will be addressed in the next section.

3.2. *Large-scale model tunnel*

Experiments were also conducted in a larger-scale outdoor model tunnel with an internal cross-sectional area of $1.16 \times 1.46\,m^2$ that was constructed for the present study. The length of the outdoor tunnel was about 27 m. The inner surfaces were made of gypsum board. By comparing the measured and predicted EA as mentioned before, it was found that the gypsum board could be treated as a perfectly hard surface. The same set of equipment as before was used, except for the source for this set of measurements. Here a Renkus-Heinz PN61 loudspeaker was used as the sound source. The heights of the source and receiver were 0.2 and 0.5 m, respectively above the bottom plane of the rectangular tunnel.

The source and receiver were placed at different positions along the tunnel. The SPLs were measured at various source/receiver configurations. The separation between the source and receiver was fixed at 10 m. Both of them were placed at a distance of 0.2 m from one of the vertical boundaries. The portion of the ground that was covered with fiberglass was altered. The discontinuity position y_D varied from 1 to 9 m. Fig. 8 shows the relative SPL when the lower horizontal plane between the source and receiver is covered with different portions of fiberglass. For example, 10% of harder surface means that $y_D = 1$ m. The relative SPL is defined in this case as the SPL taken when the ground is partly covered with fiberglass, with reference to the SPL taken at the same positions with rigid ground. The results at frequency bands of 200, 400, 1250, and 1600 Hz are shown in Figs. 8(a)–(d), respectively. In Fig. 8(a), there is a good fit of data by the coherent model from 10% to 50%

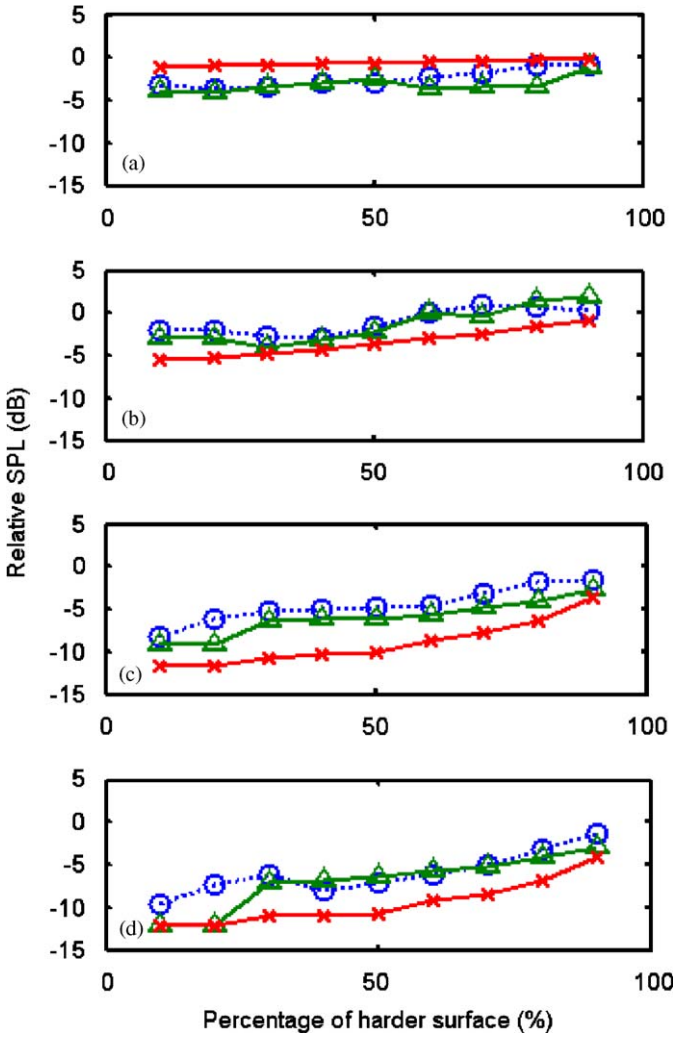

Fig. 8. Comparison of measured and predicted relative SPL at different percentages of harder surface on the ground. Source at (0.2, 0, 0.2); receiver at (0.2, 10, 0.5). Measurement: circles; coherent prediction: triangles; incoherent prediction: crosses. (a) 200 Hz; (b) 400 Hz; (c) 1250 Hz; and (d) 1600 Hz.

of hard ground. In Fig. 8(b)–(d), the coherent predictions follow the trend for the relative SPL, varying with the change of percentage of hard ground. The relative SPL is directly proportional to the percentage of hard ground. When the fiberglass coverage increases, the relative SPL decreases, indicating sound attenuation caused by the absorption material. This phenomenon is also shown in the incoherent prediction, but it is not as close to the measurement data as the coherent model. The average errors of the coherent and incoherent models are 1.83 and 3.14 dB, respectively. The predictions can also give a good approximation at other frequency bands and other source/receiver configurations, but they are not shown here for brevity.

The measured and predicted EDT spectra are compared in Fig. 9. For the data shown in Fig. 9(a), the source and receiver are placed at the centerline, i.e., 0.58 m from both vertical walls. They are separated by 16 m, and the impedance discontinuity occurs at 10 m. The downward slope between 250 and 500 Hz, and also the trend between 500 and 1000 Hz, are predicted by the coherent model. The coherent predictions are also close to the measurements at other frequency bands. In Fig. 9(b), the source–receiver distance is 10 m, and the impedance changes at $y = 7$ m. The coherent model gives an accurate prediction of the shape from 250 to 2000 Hz. The predictions from the incoherent model cannot predict the trend of the EDT spectra. It only gives

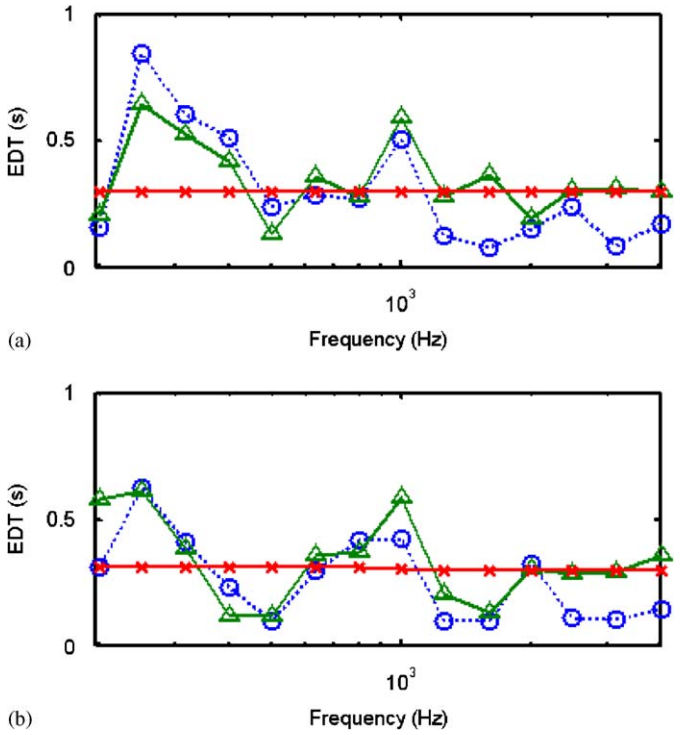

Fig. 9. Measured and predicted EDT spectra in model tunnel. Measurement: circles; coherent prediction: triangles; incoherent prediction: crosses. (a) Source at (0.58, 0, 0.2), receiver at (0.58, 16, 0.5), $y_D = 10$ m; (b) source at (0.2, 0, 0.2), receiver at (0.2, 10, 0.5), $y_D = 7$ m.

an average value of the EDT. The results from the two models are close at frequency bands above 2000 Hz. The average error of the coherent model is 0.15 s.

4. Application: strategic positioning of sound absorption materials

Kang [27,28] studied sound attenuation in long enclosures by computer simulation with the incoherent model. He suggested that the absorbers should be evenly arranged in a section in order to obtain a higher attenuation. In his analysis, the sound absorption materials were located along the entire length of the long enclosure. There was no change of impedance on the four boundaries. He also pointed out that the angle dependence of absorption coefficients, which was not included in his prediction model, was an important factor. The coherent model, which considers the angle-dependent absorption coefficient and the boundaries with mixed impedance, is now used to study the performance of absorption materials in a long enclosure.

4.1. Effect of the pattern of sound absorption material on noise reduction

A fixed amount of sound absorption material is placed on the lower horizontal plane in an imaginary long enclosure. The same 3-cm thick fiberglass is chosen to line the tunnel (where its width and height are assumed to be 6 and 4 m, respectively) in the following numerical studies. The source and receiver are placed inside the enclosure and separated by 50 m. The fiberglass covers 40% of the ground area between the source and receiver. As shown in Fig. 10, five different locations for mounting the fiberglass are investigated in our numerical analyses. Without loss of generality, all strips of fiberglass are assumed to be mounted on the bottom surface. The other three walls of the rectangular enclosure are modeled as perfectly hard surfaces.

Numerical results are presented in terms of the noise reduction, which is defined as the difference between the predicted SPL with (SPL_W) and without ($SPL_{W/O}$) the fiberglass lining:

$$NR = SPL_W - SPL_{W/O}. \tag{6}$$

The noise reduction spectra predicted in the five scenarios are shown in Fig. 11. The performance of the fiberglass in cases A and B are identical, as the noise reduction spectra are exactly the same. The five cases show similar results below 400 Hz. Case C gives an extra reduction of 1 dB at 50–80 Hz, and there is a sudden drop at 500 Hz. The results of cases C and D are similar above the frequency band of 630 Hz. However, it is obvious that the other three cases give an extra reduction of 2–3 dB at this frequency range.

The noise reduction expressed in A-weighted SPL for Cases A–E are −10.8, −10.8, −8.1, −10.7, and −8.1 dB(A). It is seen that the fiberglass achieves higher noise reduction efficiency when it is placed in a continuous length instead of being cut into strips. Moreover, the exact location at which a certain amount of absorption material is mounted in the enclosure is relatively unimportant in this particular example.

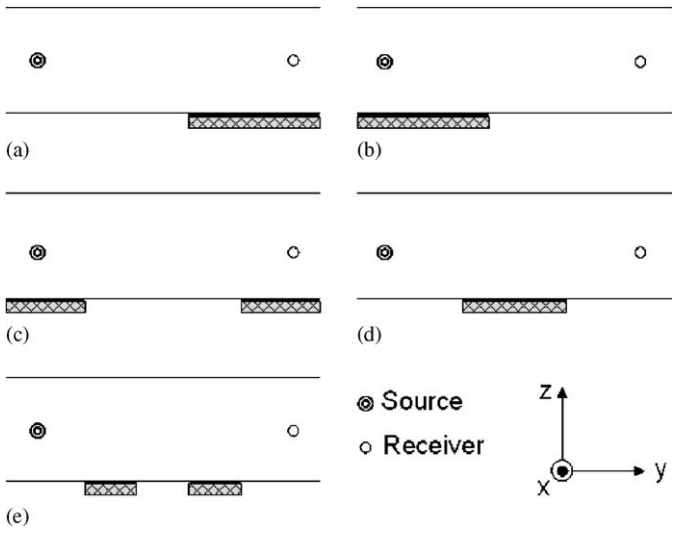

Fig. 10. Different geometries in long enclosure for five cases: (a) Case A; (b) Case B; (c) Case C; (d) Case D; and (e) Case E.

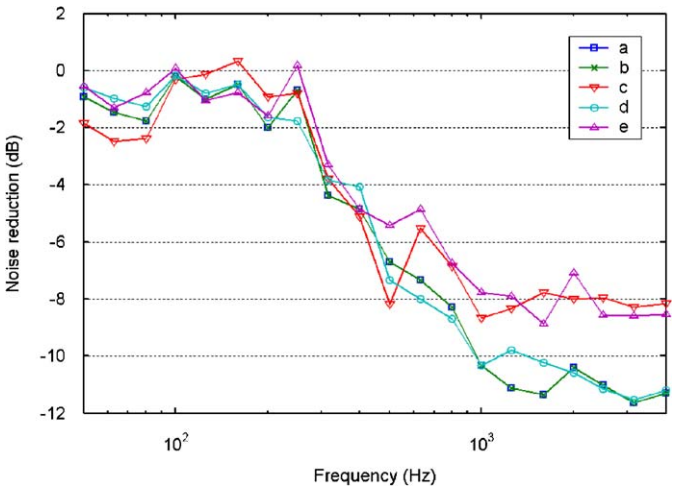

Fig. 11. Plot of relative SPL in a long enclosure with five different patterns of sound absorption material: (a) Case A; (b) Case B; (c) Case C; (d) Case D; and (e) Case E.

4.2. Effect of the amount of sound absorption material on noise reduction

It is generally assumed that an increase in the area of the sound absorption material will cause a higher level of noise reduction in a room. However, Boulanger et al. [16] examined the propagation of sound over mixed-impedance ground and found that the frequency of the EA first dip was predicted to be the highest at approximately 70% hard surface cover rather than the expected 100%. In this paper, the effect of the amount of sound absorption material on noise reduction in a long enclosure will be studied using the coherent model.

Three different cases will be explored. The geometry of the imaginary long enclosure in Case 1 is identical to the one shown in Fig. 4. The ground of the long enclosure is partly covered with fiberglass. In the second case, the ceiling of the long enclosure is also lined with sound absorption material. In the third case, only the ground and the left vertical wall are covered with sound absorption material. The distance between source and receiver is 50 m.

The noise reduction spectra for Case 1 are plotted in Fig. 12(a). For ease of comparison, not all the spectra from 10% to 100% fiberglass coverage are shown. The results are similar below the frequency band of 160 Hz. The noise reduction effect is significant when the fiberglass coverage changes from 10% to 20%. The reduction in SPL is almost double. From 30% to 50% coverage, the results obtained are similar. Further reduction is achieved at 60% coverage. It is interesting to find that between 800 and 4000 Hz, the noise reduction at 70% coverage of fiberglass is close to that at 100% coverage. This is due to the interference effects of the direct and reflected waves. When the fiberglass coverage is increased to 80%, the result is similar to that at 60%.

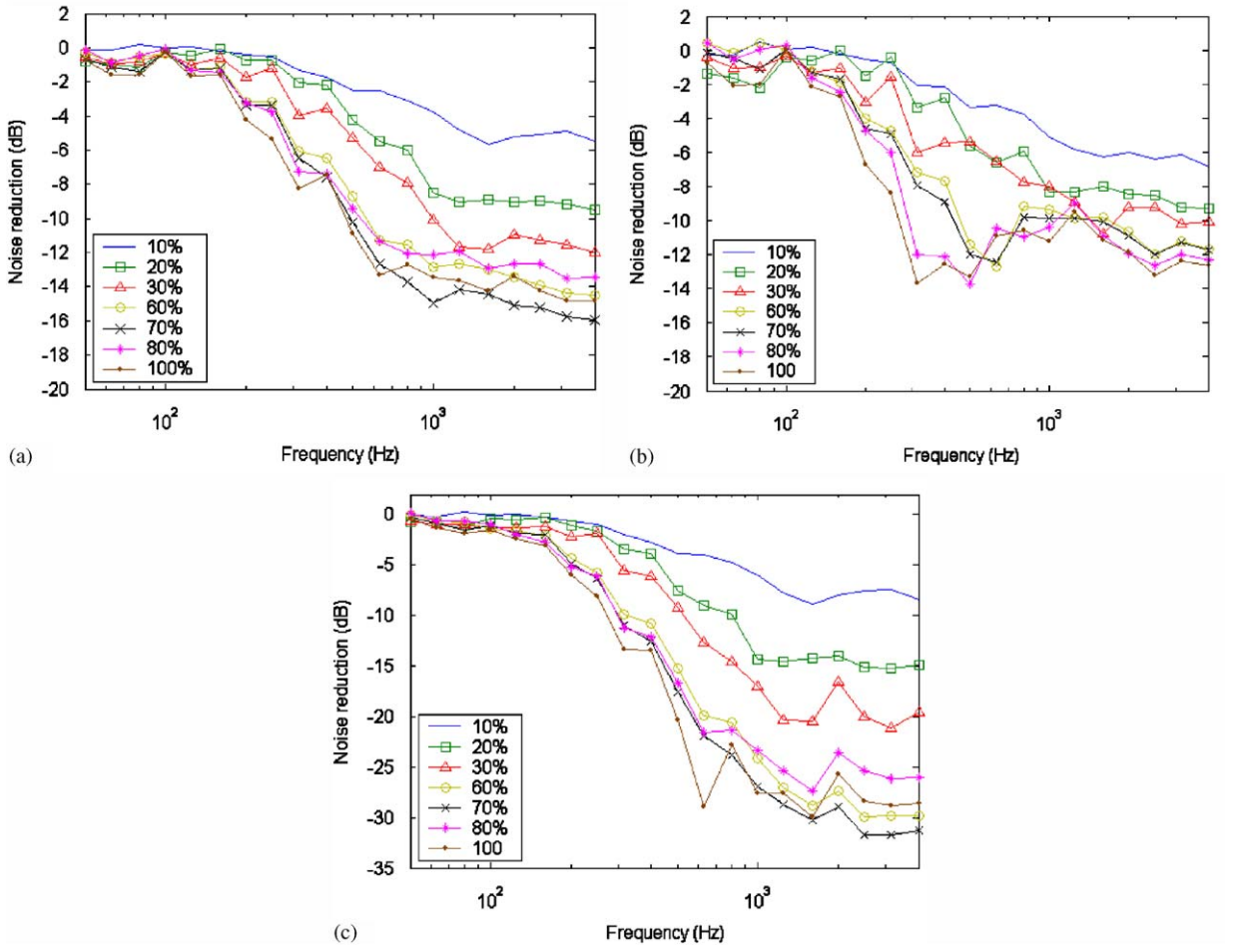

Fig. 12. Plots of noise reduction spectra in a long enclosure: (a) Case 1; (b)Case 2; and (c) Case 3.

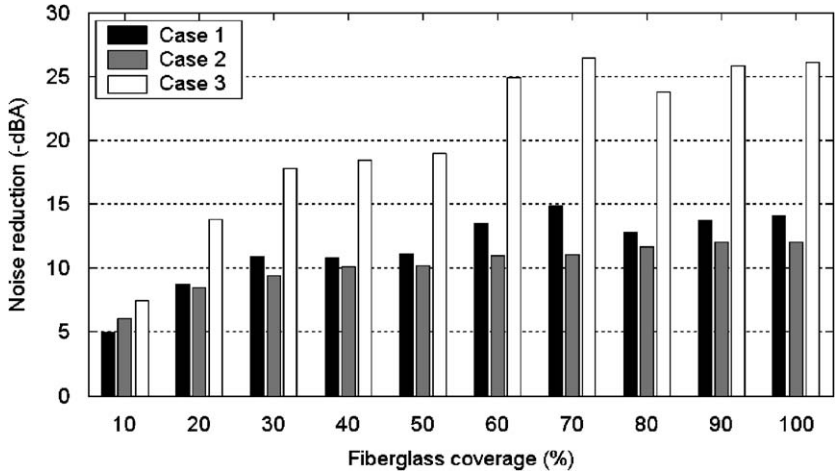

Fig. 13. Noise reduction in A-weighted SPL in a long enclosure.

When the fiberglass is used to line the ground and the ceiling in Case 2, the predicted noise reduction spectra are changed. Fig. 12(b) shows the noise reduction spectra. Maximum noise reduction is found with 100% fiberglass coverage, whereas the performance with 60% and 70% fiberglass coverage are similar now. Dips are found at 80% and 100% coverage between 250 and 1000 Hz. There is no significant extra noise reduction observed when compared to Case 1. The fiberglass lining on the horizontal planes is effective.

In the third case, the fiberglass is modeled to be placed on the ground and the left vertical wall. The predicted noise spectra for the different percentages of fiberglass coverage are shown in Fig. 12(c). The shape of the curves is similar to that in Fig. 12(a). The amount of noise reduction is increased. Noise reductions for frequencies above 1250 Hz at 70% and 100% fiberglass coverage are similar. The performance with fiberglass coverage of 60% is also marginally better than that with a coverage of 80% in this frequency range.

The noise reduction expressed in A-weighted SPL of the three cases is shown in Fig. 13. The amount of noise reduction is proportional to the amount of fiberglass lining in Case 2. However, noise reduction at 70% fiberglass coverage is found to be rather similar to that at 100% coverage in Cases 1 and 3. Furthermore, the noise reduction at 60% fiberglass coverage is marginally higher than that at 80% in these two cases. On the other hand, when the fiberglass is to be lined on two boundary surfaces to increase the noise reduction, it may be a better choice to place them on planes perpendicular to each other.

The results presented in this section provide a preliminary study of the performance of the coherent model. Further analysis can be conducted by changing the source/receiver geometry, the choice of the absorption material and its location in the long enclosure.

5. Conclusions

A theoretical model for the prediction of the sound field in two parallel horizontal planes with an impedance discontinuity is introduced. The diffraction term described in the De Jong model is implemented. Analysis is done to study the diffraction effect on the computation, and comparisons are made with predictions from another theoretical model. It is shown that the diffraction at the point of impedance change is not important in the prediction of the sound field. When the diffraction coefficients are ignored, the formulation is simplified and the computational time is greatly reduced.

The coherent model is then extended to account for the case of sound propagation in a long enclosure with a single impedance discontinuity, and an experimental validation is given. It is demonstrated that the coherent model produces results in excellent agreement with the experimental data collected, even when the diffraction at the impedance discontinuity is ignored. The accuracy of the coherent model is shown to be greater than that of the incoherent model, because the mutual interference between the source and the receiver is included.

An example of the practical usage of the coherent prediction scheme has been given. The efficiency of the installation of sound absorption material is studied with the coherent model. The absorption material is found to be more effective when it is placed in a continuous length instead of being cut into two sections in this particular case. It is also found that a higher level of noise reduction caused by an extra amount of absorption material may not be easy to observe when the percentage of covered surface is relatively large. In the examples given in this paper, fiberglass and carpet are chosen as the sound absorption materials. Further analysis can be made by comparing the performance of other absorbers. The coherent model serves as a helpful tool in the strategic lining of sound absorption material in a long enclosure to achieve noise reduction and other acoustic purposes. As a result, the performance and cost-effectiveness of the acoustic treatment will be greatly enhanced with the predictions from the coherent numerical model.

Acknowledgments

This research was supported in part by the Research Grants Council of the Hong Kong Special Administrative Region and the Research Committee of The Hong Kong Polytechnic University. The authors thank the MTR Corporation for providing a site to house a scale model tunnel at Heng Fa Chuen Depot. The authors are grateful to Dr. Glenn H Frommer of MTR Corporation for his encouragement and interest in this project. The hard works of William Fung, S.T. So, and T.L. Yip in designing and constructing the large-scale model tunnel are gratefully acknowledged.

References

[1] K.S. Sum, Some comments on Sabine absorption coefficient, *Journal of the Acoustical Society of America* 117 (2005) 486–489.
[2] J. Kang, Reverberation in rectangular long enclosures with diffusely reflecting boundaries, *Acta Acustica* 88 (2002) 77–87.
[3] F.P. Mechel, Theory of baffle-type silencers, *Acustica* 70 (1990) 93–111.
[4] N. Sormaz, A. Cummings, B. Nilsson, Sound attenuation in finite-length splitter silencers, *Proceedings of the Euronise 1992 meeting*.
[5] R.J. Astley, W. Eversman, Acoustic transmission in non-uniform ducts with mean flow, part II: the finite element method, *Journal of Sound and Vibration* 74 (1981) 103–121.
[6] W. Eversman, R.J. Astley, Acoustic transmission in non-uniform ducts with mean flow, part I: the method of weighted residuals, *Journal of Sound and Vibration* 74 (1981) 89–101.
[7] B.J. Tester, Ray models for sound propagation and attenuation in ducts, in the absence of mean flow, *Journal of Sound and Vibration* 27 (1973) 515–531.
[8] A. Cummings, High frequency ray acoustics models for duct silencers, *Journal of Sound and Vibration* 221 (4) (1999) 618–708.
[9] L.G. Ramer, The absorption of strips, effects of width and location, *Journal of the Acoustical Society of America* 12 (1941) 323–326.
[10] R.K. Cook, Absorption of sound by patches of absorbent materials, *Journal of the Acoustical Society of America* 29 (1951) 324–329.
[11] J.R. Pellam, Sound diffraction and absorption by a strip of absorbing material, *Journal of the Acoustical Society of America* 11 (1940) 396–400.
[12] J.-B. Park, K. Grosh, Y.-H. Kim, The effect of a periodic absorptive strip arrangement on an interior sound field in a room, *Journal of the Acoustical Society of America* 117 (2005) 763–770.
[13] D. Takahashi, Excess sound absorption due to periodically arranged absorptive materials, *Journal of the Acoustical Society of America* 86 (1989) 2215–2222.
[14] K.M. Li, K.K. Iu, Propagation of sound in long enclosures, *Journal of the Acoustical Society of America* 116 (2004) 2759–2770.
[15] B.A. De Jong, A. Moerkerken, J.D. Van Der Toorn, Propagation of sound over grassland and over an earth barrier, *Journal of Sound and Vibration* 86 (1983) 23–46.
[16] P. Boulanger, T. Waters-Fuller, K. Attenborough, K.M. Li, Models and measurements of sound propagation from a point source over mixed impedance ground, *Journal of the Acoustical Society of America* 102 (1997) 1432–1442.
[17] P.M. Lam, Prediction and abatement of noise in long enclosures, MPhil Thesis, Department of Mechanical Engineering, Hong Kong Polytechnic University, Hong Kong, 2005.
[18] M.E. Delany, E.N. Bazley, Acoustical properties of fibrous absorbent materials, *Applied Acoustics* 3 (1970) 105–116.
[19] S.I. Thomasson, Diffraction by a screen above an impedance boundary, *Journal of the Acoustical Society of America* 63 (1978) 1768–1781.
[20] K.B. Rasmussen, A note on the calculation of sound propagation over impedance jumps and screens, *Journal of Sound and Vibration* 84 (1982) 598–602.
[21] M.R. Stinson, G.A. Daigle, Surface wave formation at an impedance discontinuity, *Journal of the Acoustical Society of America* 102 (1997) 3269–3275.
[22] K.M. Li, H.Y. Wong, The acoustic performance of a cranked barrier: an approximate integral formulation, *ACTA Acustica* 91 (2005) 680–688.

[23] C.L. Chan, Numerical models for predicting sound propagation in ducts, MPhil Thesis, Department of Mechanical Engineering, Hong Kong Polytechnic University, Hong Kong, 2002.
[24] K. Attenborough, Ground parameter information for propagation modeling, *Journal of the Acoustical Society of America* 92 (1992) 418–427.
[25] D.D. Rife, J. Van der Kooy, Transfer–function measurement with maximum-length sequences, *Journal of the Audio Engineering Society* 37 (1989) 419–443.
[26] K.M. Li, T. Waters-Fuller, K. Attenborough, Sound propagation from point source over extended-reaction ground, *Journal of the Acoustical Society of America* 104 (1998) 679–685.
[27] J. Kang, Reverberation in rectangular long enclosures with geometrically reflecting boundaries, *Acta Acustica* 82 (1996) 509–516.
[28] J. Kang, Sound attenuation in long enclosures, *Building and Environment* 3 (1996) 245–253.